CAV2021
11th International Symposium on Cavitation
May 10-13, 2021, Daejon, Korea

Impact of Injector Geometry Details on Cavitation and Erosion Development in a Multi-hole Aluminum Injector Nozzle

Gina M. Magnotti[1]*, Aniket Tekawade[1], Brandon A. Sforzo[1], Alan L. Kastengren[2], Christopher F. Powell[1], Sibendu Som[1]

[1] Energy Systems Division, Argonne National Laboratory, United States of America
[2] X-ray Science Division, Argonne National Laboratory, United States of America

Abstract: Recent x-ray measurements performed at Argonne have demonstrated the ability to visualize erosion damage within a multi-hole injector and revealed material damage in all orifices. To understand the impact of injector geometry features on internal flow development and injector exit conditions, multiphase flow simulations of flow within different injector configurations were performed. In the non-eroded injector, the sharp inlet corner into the orifice is observed to induce high cavitation intensity levels in the first third of the orifice. At the orifice exit, no cavitation is predicted and a symmetric velocity profile is observed. In contrast, lower levels of cavitation are observed at the orifice inlet of the eroded injector due to the local area expansions and pressure losses. Due to asymmetries in the erosion patterns on the upper and lower orifice surfaces, a higher velocity core is observed towards the bottom of the orifice, which results in an asymmetric velocity profile. Overall, the erosion patterns in the orifice were predicted to induce up to a 2% decrease in the injection velocity and fuel flow rate relative to the baseline geometry at the 500 bar injection pressure tested in this study.

Keywords: automotive; fuel injector; cavitation-induced erosion; large eddy simulation

1. Introduction

To comply with regulation standards, direct injection engines have steadily increased injection pressure. However, these conditions can lead to erosion in fuel injectors and reduced performance [1]. Manufacturers must certify engine emissions for their full useful lives, and the need to minimize injector wear can often preclude running under the most efficient operating conditions. To develop accurate models for injector durability, researchers at Argonne National Laboratory carried out a joint experimental and computational study of the impact of erosion on injector performance.

This work aims to elucidate the impact of internal geometry details on cavitation erosion development and the injector exit flow conditions. First, internal flow simulations were performed on a non-eroded injector, which represents the reference geometry prior to endurance testing. Using CTSegNet [2], a new software toolkit for x-ray image processing, high-resolution x-ray scans of the eroded injector were processed into a 3D geometry and used for internal flow simulations. The predicted flow development between the non-eroded and eroded injector geometries are then analyzed to draw conclusions about the impact of geometry details on the predicted cavitation erosion and injection conditions.

2. Computational Model Set-up

In order to evaluate the impact of local geometry changes due to erosion on the internal flow development, multiphase flow simulations were performed in the baseline and eroded injectors. The

* Corresponding Author: Dr. Gina M. Magnotti, gmagnotti@anl.gov

eroded injector surfaces were generated from the x-ray image analysis workflow described in Tekawade et al. [2]. Surface details inside the aluminum injector tip are visualized in Figure 1(a), including a swirl pattern in the sac from the machining process and erosion patterns along the length of the orifices. Reference x-ray scans were not performed prior to injector endurance testing. As a result, the eroded injector geometry was used to infer the non-eroded injector geometry. Because erosion patterns are only observed in the orifices, the x-ray scanned sac and orifice inlet surfaces were stitched to the nominal orifice geometry. This process yielded an "x-ray informed" geometry, as shown in Figure 1(b), which was used to simulate the non-eroded injector case. The computational set-up for modeling pressurized fuel through an injector has been validated by the authors in previous publications [3-5], but the salient details are summarized here.

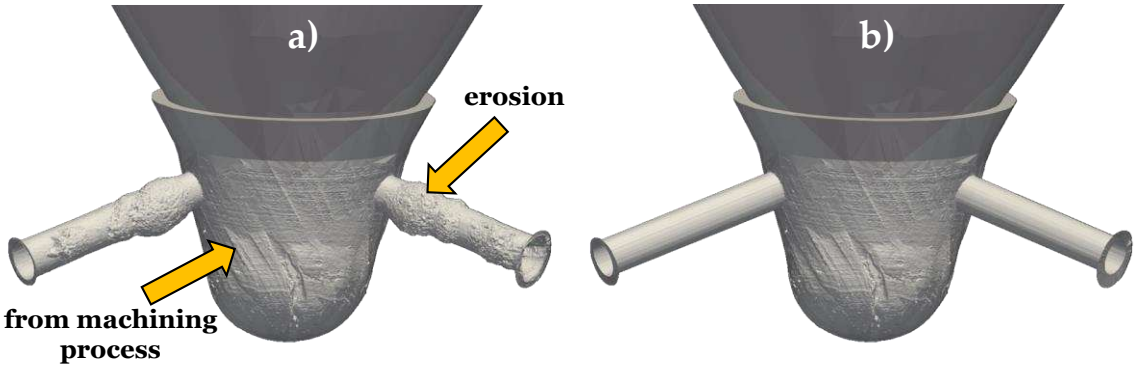

Figure 1. The transient injection event is represented by applying a moving boundary condition to the injector needle. The needle lift profile is shown in (a). The modeled domain and grid refinement strategy is shown in (b).

2.1. Injector Configuration and Operating Conditions

Using the commercially available code CONVERGE [6], internal flow simulations were performed for pressurized liquid n-dodecane fuel in the non-eroded and eroded A-M3 injectors. The A-M3 injector is geometrically similar to the Spray Combustion Consortium (SCC) M1 injector from the work of Yasutomi et al. [7]. However, instead of featuring five holes, the A-M3 injector has three side-oriented holes that are nominally oriented at an angle of 73° with respect to the needle axis and are characterized by a sharp inlet radius of curvature to promote cavitation. The transient nature of the approximately 1 ms injection event was captured with a moving boundary condition for the needle based on the measured needle lift profile.

The injection condition and fuel properties studied in this work are listed in Table 1. The fuel is liquid n-dodecane at a temperature of 323 K, which is injected at a pressure of 500 bar into a nitrogen-filled chamber with an ambient pressure of 1 bar. Dissolved gas in the fuel is represented using a trace amount of non-condensable gas species (Y_{N2} = 2e-05) in the fuel, based on recommendations from Battistoni et al. [8].

Table 1. Summary of the injection condition and fuel properties studied in this work.

Fuel	Injection Pressure	Ambient Pressure	Fuel Temperature	Saturation Pressure	Bulk Modulus	Reference Fuel Density
n-dodecane	500 bar	1 bar	323 K	133.3 Pa	1.475 GPa	727.4 kg/m^3

* Corresponding Author: Dr. Gina M. Magnotti, gmagnotti@anl.gov

2.2. Internal Flow Modeling Approach

A complete model description can be found in previous work by the author [9-10], but the key details are summarized here. The cavitating flow within the injector is treated as a compressible, homogeneous, multiphase mixture of four components and two phases: liquid and vapor fuel, non-condensable gas, and ambient gas. The transient simulation methodology for the multiphase mixture is based on the solution of the filtered form of the conservation equations of mass, momentum, and species. Turbulence closure is achieved using the Large Eddy Simulation (LES) technique, which allows for large-scale turbulent structures to be resolved while the impact of small-scale eddies on the flow is modeled. To characterize the effects of sub-grid scale turbulence, a one-equation dynamic structure model [11] is employed. The gas phase is described by the Redlich-Kwong equation of state and the liquid phase is treated as a compressible barotropic fluid. A variable time-step algorithm with a maximum acoustic-based Courant-Friedrichs-Lewy (CFL) number of 0.35 results in time steps on the order of 1 ns. A minimum mesh size of 2.5 μm is applied at the boundaries of the orifice and needle seat region, based on a grid-convergence study reported in [12]. This grid refinement strategy results in a simulation with a peak cell count of over 13 million, which requires approximately 1440 CPU-hours per 10 μs of simulated time.

3. Results

Using the non-eroded and eroded injector geometries, multiphase flow simulations were performed to contrast the cavitation and erosion development. A comparison of the cavitation development in the injector is shown in Figure 2. In the non-eroded injector, the sharp inlet corner into the orifice is observed to induce high cavitation intensity levels in the first third of the orifice. However, at the orifice exit no cavitation is observed. In contrast, lower levels of cavitation are observed in the eroded injector due to the local area expansions and pressure losses. Due to the erosion patterns in the orifice, local cavitation formation is observed and predicted to affect the injection conditions.

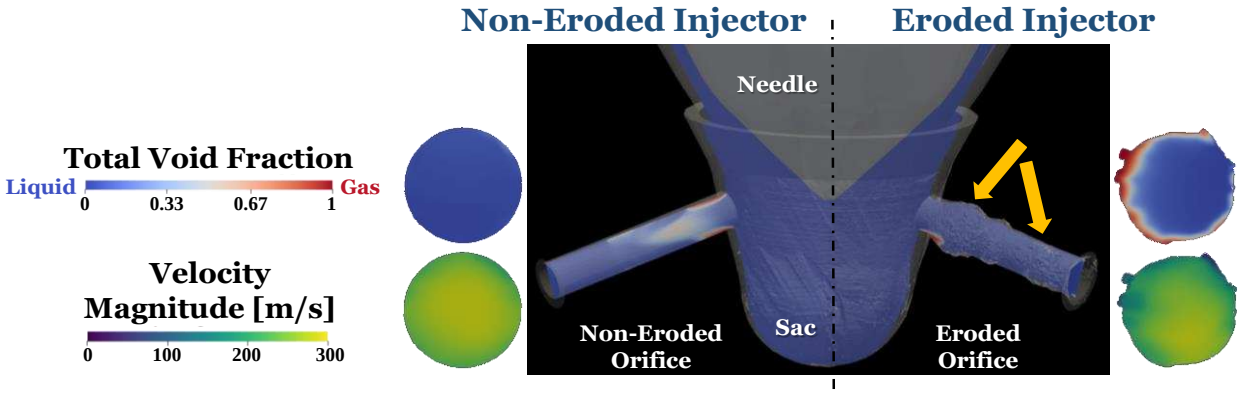

Figure 2. High-resolution x-ray scans of an eroded multi-hole injector conducted at Argonne's Advanced Photon Source revealed erosion damage in the injector orifices, as indicated by the yellow arrows. Comparison of the predicted injection conditions from the non-eroded orifice (left) and eroded orifice (right) highlight the impact of erosion on cavitation formation, injection velocity, and ultimately fuel delivery rate.

A comparison of the injection conditions, based on the predicted total void fraction and velocity magnitude at the orifice exit, is also shown in Figure 2. In general, comparatively lower injection velocities

* Corresponding Author: Dr. Gina M. Magnotti, gmagnotti@anl.gov

are observed for the eroded injector. The cause of this difference can be found by evaluating the predicted flow development along the length of the non-eroded and eroded orifices, as shown in Figure 3. In the non-eroded geometry, the local area contraction at the orifice inlet results in cavitation formation and local flow acceleration, as shown in Figure 3 (a) and (c), respectively. Downstream of the orifice inlet, the velocity profile decelerates but maintains a relatively constant profile across the diameter of the orifice. In contrast, although the flow accelerates in the first 5% of the eroded orifice length, as highlighted in Figure 3(d), the local area expansion due to erosion results in a large pressure loss and deceleration of the flow. Due to the asymmetries in the erosion profile, a higher velocity core is observed towards the bottom of the orifice and results in an asymmetric injection profile, as shown in Figure 2. Overall, the erosion patterns in the orifice led to a 2% decrease in the predicted injection velocity and fuel flow rate relative to the baseline geometry.

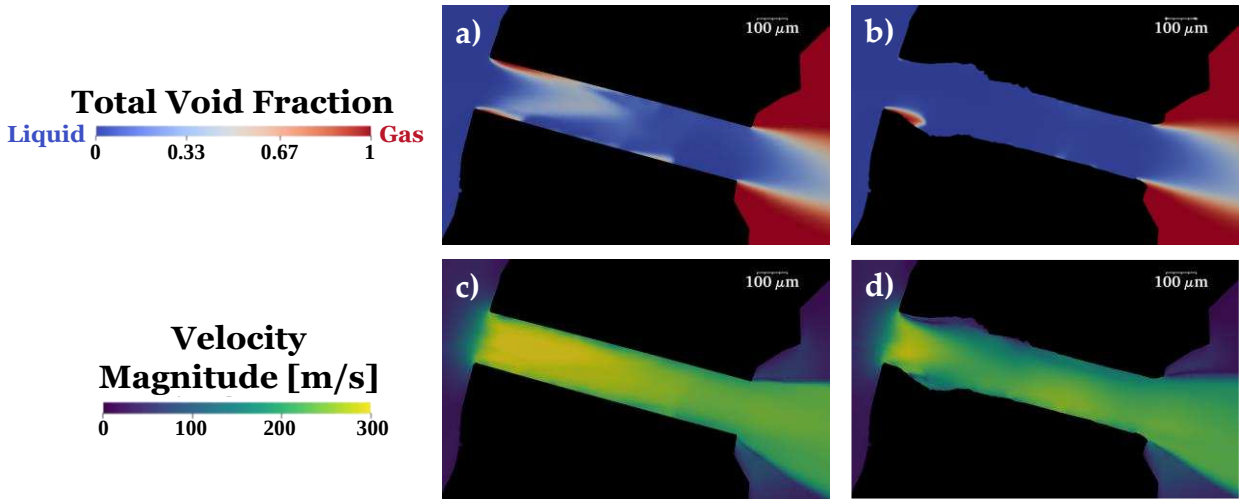

Figure 3. A comparison of the predicted flow development for (a-b) total void fraction and (c-d) velocity magnitude distributions for the non-eroded and eroded injector geometries respectively. The visualizations are shown along the central slice at the time instant of maximum needle lift.

Acknowledgments: The submitted manuscript has been created by UChicago Argonne, LLC, Operator of Argonne National Laboratory (Argonne). Argonne, a U.S. Department of Energy Office (DOE) of Science laboratory, is operated under Contract No. DE-AC02-06CH11357. The U.S. Government retains for itself, and others acting on its behalf, a paid-up nonexclusive, irrevocable worldwide license in said article to reproduce, prepare derivative works, distribute copies to the public, and perform publicly and display publicly, by or on behalf of the Government.

Argonne National Laboratory's work was supported by the U.S Department of Energy under contract DE-AC02-06CH11357. The authors gratefully acknowledge the computing resources provided on Bebop, a high-performance computing cluster operated by the Laboratory Computing Resource Center at Argonne National Laboratory, and Convergent Science Inc., for providing the CONVERGE CFD software licenses. X-ray experimental data presented in this paper were acquired at the 7-BM beamline of the Advanced Photon Source (APS) at Argonne National Laboratory. Use of the APS is supported by the U.S. Department of Energy (DOE) under Contract No. DE-AC0-206CH11357.

References

1. Tzanetakis, T., Traver, M., Costanzo, V., Medina, R. et al., "Durability Study of a High Pressure Common Rail Fuel Injection System Using Lubricity Additive Dosed Gasoline-Like Fuel - Additional Cycle Runtime and Teardown Analysis," *SAE Int. J. Adv. & Curr. Prac. in Mobility* 1(2):654-674, 2019, https://doi.org/10.4271/2019-01-0263.

* Corresponding Author: Dr. Gina M. Magnotti, gmagnotti@anl.gov

2. Tekawade, A. et al., "High-fidelity geometry generation from CT data using convolutional neural networks," Proc. SPIE 11113, Developments in X-Ray Tomography XII, 111131X (10 September 2019); https://doi.org/10.1117/12.2540442.
3. Battistoni, M., Som, S., and Powell, C.F., "Highly resolved Eulerian simulations of fuel spray transients in single and multi-hole injectors: Nozzle flow and near-exit dynamics," *Fuel*, 251:709-729, 2019. https://doi.org/https://doi.org/10.1016/j.fuel.2019.04.076
4. Torelli, R. et al., "Influence of fuel properties on internal nozzle flow development in a multi-hole diesel injector," *Fuel*, 204:171-184, 2017. https://doi.org/10.1016/j.fuel.2017.04.123.
5. Torelli, R., Magnotti, G.M., Som, S., Pei, Y. et al., "Exploration of Cavitation-Suppressing Orifice Designs for a Heavy-Duty Diesel Injector Operating with Straight-Run Gasoline," SAE Technical Paper 2019-24-0126, 2019, doi:10.4271/2019-24-0126.
6. Richards, K. J., Senecal, P. K., and Pomraning, E., CONVERGE 3.0 Manual, Convergent Science, Madison, WI (2020).
7. Yasutomi, K., Hwang, J., Pickett, L.M., Sforzo, B., et al., "Transient Internal Nozzle Flow in Transparent Multi-Hole Diesel Injector", SAE Technical Paper 2020-01-0830, 2020. https://doi.org/10.4271/2020-01-0830
8. Battistoni, M., Duke, D., Swantek, A., Tilocco, F., et al., "Effects of Noncondensable Gas on Cavitating Nozzles". *Atomization and Sprays*, 25: p. 453-483, 2015. https://doi.org/10.1615/AtomizSpr.2015011076
9. Milan, P.J. et al., "Data-Driven Model Reduction of Multiphase Flow in a Single-Hole Automotive Injector", *Atomization and Sprays*, 30(6): 401-429, 2020.
10. Mondal, S. et al., "Accelerating the Generation of Static Coupling Injection Maps Using a Data-Driven Emulator," SAE Technical Paper 2021-01-0428, 2021.
11. Pomraning, E. and Rutland, C.J., "Dynamic One-Equation Nonviscosity Large-Eddy Simulation Model". *AIAA Journa*l, 40(4): p. 689-701, 2020. https://doi.org/10.2514/2.1701
12. Magnotti, G.M., Battistoni, M., Saha, K., and Som, S., "Influence of Turbulence and Thermophysical Fluid Properties on Cavitation Erosion Predictions in Channel Flow Geometries", in SAE International Journal of Advances and Current Practices in Mobility, 2(4):2229-2240, 2020.https://doi.org/10.4271/2019-01-0290

* Corresponding Author: Dr. Gina M. Magnotti, gmagnotti@anl.gov